# Comparative Analysis of Electron Cyclotron Radiation Power Losses in Tokamaks IGNITOR and ITER

P.V. Minashin[1], A.B. Kukushkin[1,2]

[1]*NRC "Kurchatov Institute", Moscow, Russia*

[2]*Nuclear Research National University MEPhI, Moscow, Russia*

**1. Introduction.** The next generation of fusion experiments will be focused on the research of plasma under ignition conditions (domination of the heating from fusion reactions for times long compared to the most important plasma characteristic time scales). Tokamak ITER, which is currently under construction in France, is the leading project in the magnetically confinement fusion contemporary physics. To demonstrate the feasibility of fusion power the ITER project has to perform two major objectives: reach an energy gain factor of Q = 10 (the ratio of the fusion power produced to auxiliary heating power) and to obtain self-sustained fusion plasma. Another proposed experiment is the IGNITOR project [1]–[4], which aims at demonstrating the possibility of the ignition achieved by the ohmic heating alone (or with minimum use of auxiliary heating). Although ITER and IGNITOR significantly differ from each other in many key parameters, the achievement of plasma ignition conditions require for both projects the increase of the magnetic field as compared to the present devices. This leads to a possible increase of the role of the electron cyclotron (EC) losses in the local electron power balance, which should be considered for optimizing the device operational scenarios.

**2. The EC power losses in tokamaks IGNITOR and ITER.** The first attempt to perform a numerical calculation of total and local net EC power losses in IGNITOR (taking into account the effects of the net absorption of the EC radiation on the periphery of the plasma column [5], [6]) was carried out in [7] for the first version of tokamak IGNITOR project (in [7] the approach [8] is used, which allowed to generalize and improve the method [5]). Figure 1 shows the EC power losses in two basic regimes of tokamak IGNITOR operation [9]. Note that the scenario 2 is close to the second scenario in the recent paper [4] (see Table 1 in [4], the results for the spatial distribution of the main parameters in [4] are not available). The calculations were carried out with numeric codes CYNEQ [7], [10] (using the modified version CYNEQ-B (1D) [11] (account of plasma equilibrium effects)) and CYTRAN [5].

For comparison of the results for tokamak IGNITOR and ITER we show (Fig. 2) the EC power losses for two scenarios of ITER operation. The description of the main characteristics of the "inductive" regime is given in [12], "steady-state" regime — [13], [14].

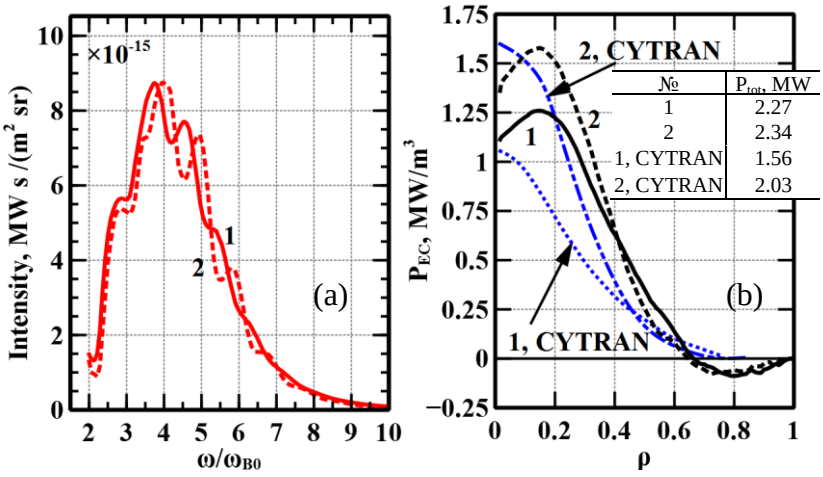


Figure 1. Comparison of the spectral intensity of the outgoing EC radiation intensity ($\omega_{B0}$ is the EC frequency for the vacuum magnetic field on torus axis) (a), spatial profiles of the EC net local losses, $P_{EC}(\rho)$, and total (volume-integrated) losses, $P_{tot}$ (b) in scenarios 1 and 2 of tokamak IGNITOR operation. Calculations are carried out with the CYNEQ-B(1D) code. The wall reflection coefficient for the EC radiation $R_w$=0.6.

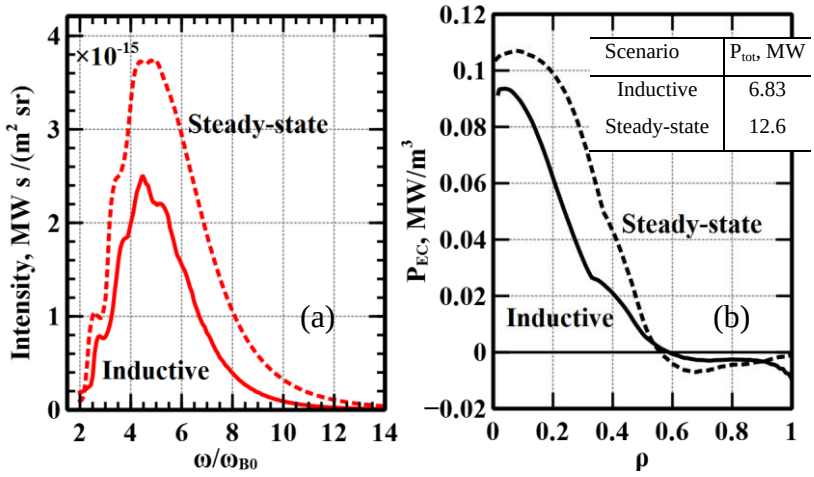


Figure. 2. The same as in figure 1 but for "inductive" and "steady-state" scenarios of tokamak ITER operation.

To assess the role of the EC power losses in IGNITOR one should compare the data of figure 1 with the other components of the electron energy balance (see Fig. 6 a, b and 6, c in [9]). It is seen that the diversification of EC power losses calculations did not affect the conclusion [9] about the role of the EC power losses: the main components of the electron energy balance are the heating by the alpha-particles and the heat losses due to anomalous electron thermal conductivity. For the "inductive" regime of ITER operation, as it follows from the results of [12], the EC power losses do not play a significant role. This conclusion is also valid for the "inductive" scenario of ITER operation according to [9] (see Fig. 4, *c* therein). The situation changes dramatically with increasing electron temperature predicted for the "steady-state" regimes of ITER operation [9]. A detailed analysis of the role of EC power losses in the "steady-state" regime of ITER operation [13] was carried out in [15], [14]: in the central plasma the EC power losses become comparable with the total auxiliary heating power and are the one third of the heating by alpha-particles (see Fig. 3 in [14]).

**3. Influence of the non-Maxwellian VDF on the EC power losses in ITER and IGNITOR.** Influence of non-Maxwellian velocity distribution function (VDF) on the EC power losses is much less analyzed than that in the case of Maxwellian plasma. In [10] the EC

radiation power losses was studied in the case of an isotropic bi-Maxwellian VDF with Gaussian distribution of effective temperatures in space coordinates. In [16] the modification of the code RAYTEC [17] is given to take into account an anisotropic non-Maxwellian VDF of electrons.

Here we use the model electron VDF:

$$f_e(\mathbf{p},\mathbf{r}) = n_e(\rho)\left\{\left[1-\delta_{n_e}(\rho)\right] f_{\mathrm{MAXW}}(\mathbf{p}, T_e(\rho)) + \delta_{n_e}(\rho)\, f_{\mathrm{hot}}(\mathbf{p},\mathbf{r})\right\}, \quad (1)$$

where the electrons of the thermal plasma component are described by the relativistic Maxwellian VDF $f_{MAXW}(\mathbf{p}, T_e)$, and the super-thermal electrons by a model anisotropic VDF:

$$f_{\mathrm{hot}}(\mathbf{p},\ \mathbf{r}) = A\cdot\exp\left[-m_e c^2\left(\sqrt{1+\frac{p_\perp^2}{(m_e c)^2}+\frac{p_\parallel^2}{(m_e c)^2}}-1\right)\left(\frac{\sin^2\theta_p}{T_\perp(\rho)}+\frac{\cos^2\theta_p}{T_\parallel(\rho)}\right)\right], \quad (2)$$

here A is normalization factor, $p_{\perp,\parallel}$ are the components of electron momentum perpendicular and parallel to magnetic field. Spatial distributions of the density and temperature profiles of the super-thermal electrons are given by Gaussian distributions:

$$\delta_{n_e}(\rho) = \delta_{n_e}^{\max}\exp[-(\rho-\rho_0)^2/(\Delta\rho)^2], \quad (3)$$

$$T_{\perp,\parallel}(\rho) = T_{\perp,\parallel}^{\max}\exp[-(\rho-\rho_0)^2/(\Delta\rho)^2], \quad (4)$$

where parameters $\rho_0$, $\Delta\rho$ are taken from [12-13]. The results are given in Figures 3-4.

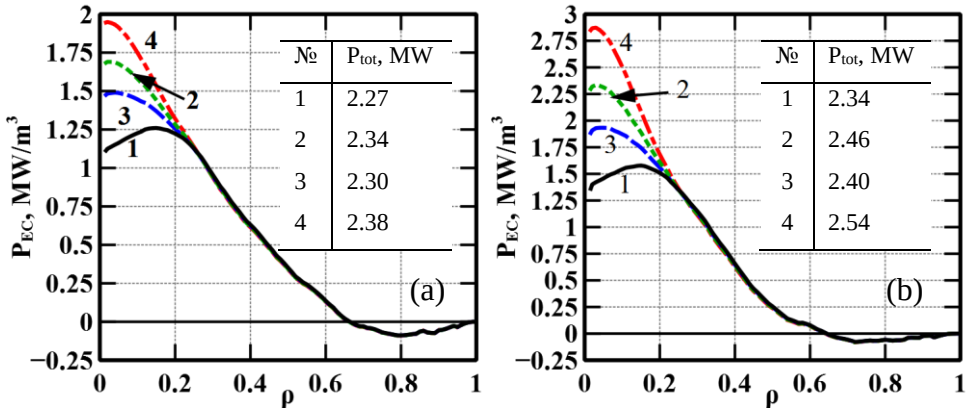


Figure 3. Spatial profile of the EC net local losses, $P_{EC}(\rho)$, and total power losses, $P_{tot}$, for the IGNITOR scenarios 1 ($I_p$ = 7 MA) (a) and 2 ($I_p$ = 11 MA) (b) for the Maxwellian VDF (1), isotropic VDF for super-thermal electrons with $T_\parallel^{\max} = T_\perp^{\max} = 3T_e(0)$ keV (2), anisotropic bi-Maxwellian VDF with $T_\parallel^{\max} = 3T_e(0)+10$ keV, $T_\perp^{\max} = 3T_e(0)-10$ keV (3), anisotropic bi-Maxwellian VDF with $T_\parallel^{\max} = 3T_e(0)-10$ keV, $T_\perp^{\max} = 3T_e(0)+10$ keV (4). Spatial distribution of the density and temperature profiles of the super-thermal electrons are taken the Gaussians with $\rho_0 = 0$, $\Delta\rho = 0.27$, $\delta_{n_e}^{\max} = 0.01$. Calculations are carried out with the CYNEQ-B(1D) code.

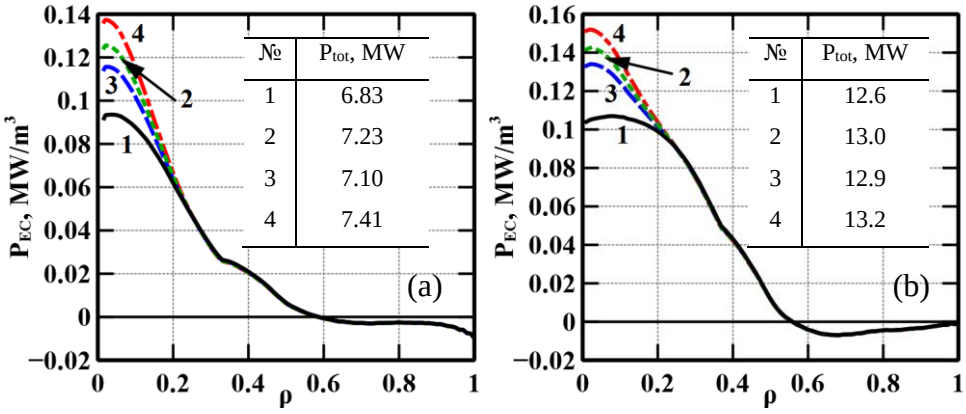


Figure 4. The same as in figure 3 but for the "inductive" (a) and "steady-state" (b) regimes of ITER operation.

**4. Conclusions.** In the present paper we made a comparative analysis of the role of the EC power losses in tokamaks IGNITOR and ITER. The analysis is carried out with the CYNEQ code [7], [10], using the modified version of the CYNEQ-B(1D) code [11]. Although ITER and IGNITOR significantly differ in many key parameters, the relevance of the comparative analysis is related to the use of the high magnetic field (compared to existing devices) to achieve ignition conditions. We demonstrate that despite the strong magnetic field, the EC radiation power losses in tokamak IGNITOR do not play a significant role in the local electron plasma energy balance and do not influence the plasma ignition conditions.

## References

[1] B. Coppi *et al.*, Nuclear Fusion **41**, 1253-7, (2001)
[2] A. Airoldi and G. Cenacchi, Nuclear Fusion **37**, 1117-27, (1997)
[3] A. Airoldi and G. Cenacchi, Nuclear Fusion **41**, 687-93, (2001)
[4] B. Coppi *et al.*, Nuclear Fusion **53**, 104013, (2013)
[5] S. Tamor, Science Applications, Inc. Report SAI-023-81-189LJ/LAPS-72 (1981)
[6] S. Tamor, Nuclear Technology/Fusion **3**, 293, (1983)
[7] A.B. Kukushkin, *Proc.* 14th IAEA Conference on Plasma Physics and Controlled Nuclear Fusion Research (Wuerzburg, Germany) 2 (IAEA), 35-45 (1992)
[8] A.B. Kukushkin, JETP Letters **56**, 487, (1992)
[9] F. Albajar *et al.*, Nuclear Fusion **45**, 642-8, (2005)
[10] K.V. Cherepanov and A.B. Kukushkin, *Proc.* 20th IAEA Fusion Energy Conference (Vilamoura, Portugal) TH/P6-56 (2004)
[11] A.B. Kukushkin and P.V. Minashin, *Proc.* 36th EPS Conference on Plasma Physics (Sofia, Bulgaria) 33E (ECA), P-4.136 (2009)
[12] A.R. Polevoi *et al.*, Journal of Plasma and Fusion Research SERIES **5**, 82-7, (2002)
[13] A.R. Polevoi *et al.*, *Proc.* 37th EPS Conference on Plasma Physics (Dublin, Ireland) 34A (ECA), P2.187 (2010)
[14] A.B. Kukushkin, P.V. Minashin and A.R. Polevoi, Plasma Physics Reports **38**, 211-20, (2012)
[15] A.B. Kukushkin, P.V. Minashin and A.R. Polevoi, *Proc.* 23rd IAEA Fusion Energy Conference (Daejon, South Korea) ITR/P1-34 (2010)
[16] F. Albajar, M. Bornatici and F. Engelmann, *Proc.* 16th Joint Workshop "Electron Cyclotron Emission And Electron Cyclotron Resonance Heating" (Sanya, China) 215-21 (2010)
[17] F. Albajar, M. Bornatici and F. Engelmann, Nuclear Fusion **49**, 115017, (2009)